Am J Cancer Res 2025;15(12):5199-5212
www.ajcr.us /ISSN:2156-6976/ajcr0164899

*Original Article*

# Macrophage-derived exosomes induce M2 microglial polarization to alleviate bone cancer pain

Jiaxin Xie[1,2*], Libiao Yuan[1*], Jiyan Li[1], Yaping Liu[3], Xiangming Li[1], Zhiqiang Dai[2], Weixing Ding[4], Zhangxiang Huang[1]

[1]*Department of Pain, First Affiliated Hospital of Kunming Medical University, Kunming 650000, Yunnan, China;* [2]*Department of Neurosurgery, The 920th Hospital of Joint Logistics Support Force of The Chinese People's Liberation Army, Kunming 650000, Yunnan, China;* [3]*Department of Eye, Kunming Tongren Hospital, Kunming 650000, Yunnan, China;* [4]*Department of Pain, Qujing Second People's Hospital, Qujing 655009, Yunnan, China.* [*]*Equal contributors.*

Received March 29, 2025; Accepted October 13, 2025; Epub December 15, 2025; Published December 30, 2025

**Abstract:** Bone cancer pain (BCP) is a frequent and debilitating complication in patients with malignant tumors, arising from a multifactorial interplay of bone destruction, neural injury, and inflammatory responses. Microglia can polarize into either an M1 phenotype, which aggravates nociception, or an M2 phenotype, which facilitates pain resolution. Activation of the TLR4/NF-κB signaling cascade is known to drive M1 polarization, thereby amplifying inflammation and neuronal damage. This study aimed to investigate whether macrophage-derived exosomes could mitigate BCP by modulating the TLR4/NF-κB pathway, suppressing M1 polarization, and enhancing M2 microglial polarization. *In vitro*, RAW264.7 macrophages were polarized to the M2 phenotype via IL-4 stimulation, and exosomes were subsequently isolated and applied to LPS-challenged BV2 microglial cultures. Polarization profiles were analyzed using flow cytometry, immunofluorescence, qRT-PCR, and Western blotting. *In vivo*, a rat BCP model was established, and exosome treatments were administered. Behavioral assays were performed to assess pain responses, followed by evaluation of microglial polarization and TLR4/NF-κB pathway activity in spinal cord tissue. Results demonstrated that IL-4 treatment effectively induced M2 polarization in RAW264.7 cells, and the isolated exosomes displayed characteristic morphology and marker expression. BV2 microglia internalized these vesicles, leading to pronounced inhibition of LPS-induced M1 polarization, promotion of M2 polarization, suppression of pro-inflammatory cytokine release, and downregulation of TLR4/NF-κB activation. *In vivo*, exosome administration elevated the mechanical pain threshold and attenuated pain-related behaviors, while spinal cord analyses revealed reduced expression of M1 markers, increased M2 markers, and marked suppression of TLR4/NF-κB signaling. Collectively, these findings indicate that macrophage-derived exosomes alleviate BCP through coordinated regulation of TLR4/NF-κB signaling and microglial polarization, suggesting their potential as a novel therapeutic option for managing bone cancer pain.

**Keywords:** Macrophage-derived exosomes, microglial polarization, TLR4/NF-κB signaling pathway, bone cancer pain, inflammation regulation

## Introduction

Bone cancer pain (BCP) is one of the most frequent and distressing complications associated with malignant tumors. As the tumor burden increases, pain symptoms often intensify, markedly diminishing a patient's quality of life [1]. The pathology of BCP is multifactorial, involving bone destruction, neural injury, and robust inflammatory responses [2]. Among the cellular mediators of this process, microglia-resident immune cells of the central nervous system- are central mediators, capable of detecting and responding to neural damage and inflammatory signals [3]. Upon activation, microglia can polarize into distinct functional phenotypes: the pro-inflammatory M1 state and the anti-inflammatory, reparative M2 state [4].

M1-polarized microglia exacerbate inflammation and tissue injury by releasing cytokines such as tumor necrosis factor-α (TNF-α), interleukin-1β (IL-1β), and IL-6, thereby intensi-

https://doi.org/10.62347/BCLF6941

fying nociceptive signaling [5]. Conversely, M2-polarized microglia contribute to inflammation resolution and tissue repair through the release of anti-inflammatory mediators, including IL-10 and transforming growth factor-β (TGF-β) [6]. In BCP, polarization is often skewed toward the M1 phenotype, creating a pro-inflammatory milieu that exacerbates pain and neuronal injury.

A key molecular driver of this imbalance is the activation of the Toll-like receptor 4/nuclear factor-κB (TLR4/NF-κB) pathway [7]. TLR4, a pattern recognition receptor, detects pathogen- or damage-associated molecular patterns (PAMPs/DAMPs) and triggers downstream NF-κB signaling [8], a canonical pro-inflammatory cascade that induces cytokine production, including TNF-α and IL-1β [9]. In BCP models, excessive TLR4/NF-κB activation preferentially induces M1 polarization, heightening pain sensitivity [10]. Therefore, modulating this pathway is crucial for suppressing M1 polarization, enhancing M2 polarization, and mitigating BCP symptoms.

Although multiple experimental approaches have targeted TLR4/NF-κB signaling, clinically effective interventions remain elusive, making novel regulatory strategies a priority. Exosomes-30-150 nm extracellular vesicles loaded with proteins, lipids, mRNAs, and miRNAs-serve as intercellular messengers capable of altering the physiological state of recipient cells [11, 12]. Accumulating evidence implicates the key role of exosomes in immune modulation and inflammation control, particularly in influencing macrophage and microglial polarization [13, 14]. Macrophage-derived exosomes, which may carry regulatory miRNAs such as miR-216a or miR-21, have been shown to promote M2 polarization and suppress M1 polarization through the delivery of anti-inflammatory cargos and suppression of pro-inflammatory signaling [15, 16]. These properties confer significant therapeutic potential in diseases driven by chronic inflammation. Indeed, exosome-based interventions have demonstrated efficacy in alleviating neuropathic and inflammatory pain by dampening pro-inflammatory pathways, modulating neuronal activity, and supporting tissue repair [17].

Building on these, we hypothesize that macrophage-derived exosomes can relieve BCP by down-regulating TLR4/NF-κB activity, inhibiting M1 and facilitating M2 microglial polarization. In this study, we assessed these effects in vitro-using IL-4-induced M2 macrophages as the exosome source and lipopolysaccharide (LPS) - stimulated microglia as targets- and in vivo, employing a rat BCP model. These experiments aim to clarify the mechanistic role of macrophage-derived exosomes in BCP modulation and provide a theoretical foundation for their development as novel analgesic biotherapeutics.

## Methods and materials

### *Cell culture and treatment*

*Culture and induction of M2 polarization in RAW264.7 cells:* RAW264.7 macrophages (ATCC) were cultured in Dulbecco's Modified Eagle Medium (DMEM) containing 10% fetal bovine serum (FBS) at 37°C in a humidified incubator with 5% $CO_2$. Once cultures reached approximately 70-80% confluence, M2 polarization was induced by treating the cells with 20 ng/mL IL-4 for 24 h. Polarization status was subsequently verified by flow cytometry, ELISA, and immunofluorescence staining, confirming a shift toward the M2 phenotype.

*Extraction and characterization of exosomes:* Exosomes were isolated from the supernatant of IL-4-treated RAW264.7 cultures via a sequential ultracentrifugation protocol. Briefly, the conditioned medium was first centrifuged at 300 × g for 10 min to remove cellular debris, followed by a 2,000 × g spin for 20 min to exclude larger vesicles. The clarified supernatant was then ultracentrifuged at 120,000 × g for 70 min to pellet the exosomes, which were resuspended in 200 μL PBS. A second ultracentrifugation step was performed to improve purity, and density gradient centrifugation was applied to further minimize contamination from non-exosomal extracellular vesicles.

Exosome morphology was assessed by transmission electron microscopy (TEM), revealing the characteristic bilayer membrane structure with diameters ranging from 50-150 nm. Nanoparticle tracking analysis (NTA) showed a predominant peak at ~100 nm and a concentration of roughly $3 \times 10^{11}$ particles/mL. Protein quantification by BCA assay yielded ~150 μg of total exosomal protein per 10 mL of culture

supernatant. Western blotting confirmed the presence of exosome-specific markers (CD63, CD81, CD9) and absence of the cytosolic protein GAPDH, verifying the successful isolation of exosomes.

*Culture and treatment of BV2 microglial cells:* BV2 microglial cells (ATCC) were cultured under the same conditions as RAW264.7 cells. To induce an inflammatory response and drive M1 polarization, BV2 cells were exposed to 1 μg/mL LPS. Following induction, macrophage-derived exosomes were introduced into the cultures and co-incubated for an additional 24 h to assess their regulatory influence on microglial polarization profiles.

*Exosome uptake assay (PKH67 Labeling):* For *in vitro* and *in vivo* uptake assessment, exosomes were labeled with the green-fluorescent dye PKH67. *In vitro*, freshly isolated exosomes were incubated with PKH67 for 5 min at room temperature, diluted with PBS, and ultracentrifuged to remove unbound dye. Labeled vesicles, resuspended in PBS at a concentration of $3 \times 10^{11}$ particles/mL, were added to BV2 cultures for 24 h.

After treatment, BV2 cells were fixed in 4% paraformaldehyde, permeabilized with 0.3% Triton X-100, and blocked with 5% BSA for 1 h. Nuclei were counterstained with DAPI. Localization of PKH67-positive vesicles was visualized under a fluorescence microscope, with detection of red fluorescence (PKH67 signal) within microglia indicating successful vesicle internalization. Uptake efficiency was quantified using dedicated image analysis software under the specified experimental conditions.

For *in vivo* tracking, PKH67-labeled exosomes (100 μg in 50 μL PBS) were administered via intrathecal injection to rats in the BCP + Exo group. After 24 hours, rats were euthanized, and lumbar spinal cord tissues were collected and fixed in 4% paraformaldehyde. Tissue sections were cryoprotected with 30% sucrose, embedded in OCT compound, and sliced into 10 μm thick sections. After permeabilization and blocking, immunofluorescence staining was performed using microglial markers (Iba1 and/or F4/80), followed by incubation with fluorescent secondary antibodies. DAPI was used for nuclear staining. Fluorescence microscopy was used to assess the colocalization of red fluorescence (PKH67-labeled exosomes) with microglia (green, Iba1) in spinal cord tissues. DAPI (blue) was used to identify cell nuclei. Red puncta overlapping with microglial regions indicated successful delivery and uptake of exosomes by microglia *in vivo*.

*Animal experiments and establishment of the bone cancer pain model*

Thirty adult male Sprague-Dawley (SD) rats, weighing between 180-220 g, were obtained from a designated animal center. All rats were acclimated for one week prior to the experiment under controlled conditions of constant temperature (22±1°C) and a 12-hour light-dark cycle. The animal experimental protocol was approved by the First Affiliated Hospital of Kunming Medical University's Animal Ethics Committee, and all procedures adhered strictly to animal ethical guidelines. The rats were randomly divided into three groups, with 10 rats per group: Sham group, BCP (Bone Cancer Pain) model group, and BCP + Exo (exosome treatment) group. The BCP model was established by inoculating Walker 256 breast cancer cells into the tibial marrow cavity. Specifically, under anesthesia with isoflurane (2%-3%), the tibial cortex was exposed, and 20 μL of a physiological saline suspension containing $1 \times 10^6$ Walker 256 cells was injected into the marrow cavity, followed by closure of the cavity. The Sham group received an injection of an equal volume of physiological saline without cancer cells. The BCP + Exo group received additional exosome exposure.

After the establishment of the BCP model, exosomes derived from M2-polarized RAW264.7 macrophages were administered to the BCP + Exo group via intrathecal injection. The exosomes were injected directly into the intrathecal space of the rats to target the spinal cord and central nervous system. A total of 100 μg of exosomes in 50 μL of PBS was administered per rat, with one injection given on the day following tumor cell inoculation and another injection at 7 days post-inoculation. Post-surgery, animals were housed under standard conditions. Euthanasia was performed at the end of the experiment using an overdose of pentobarbital sodium (150 mg/kg, intraperitoneal injection) in accordance with animal ethical standards.

*Mechanical pain threshold testing (Von Frey Filament Test)*

The mechanical nociceptive response of the rats was assessed using the von Frey filament test. Rats were placed in a metal mesh cage, and von Frey filaments were gradually applied to the hind paw until the rat exhibited a paw withdrawal response. Each rat was tested three times, and the average value was calculated as the paw withdrawal threshold (PWT). Mechanical nociceptive responses were assessed every 3 days using the von Frey filament test for a period of 18 days.

*Immunofluorescence (IF) staining*

The polarization state of BV2 cells was detected by immunofluorescence staining. BV2 cells were seeded on slides in a 24-well plate and allowed to reach 50%-60% confluence before fixation and permeabilization. Sections were blocked with 5% BSA for 1 hour at room temperature, then incubated overnight at 4°C with primary antibodies to CD206 and Arg-1. The next day, sections were washed three times with PBS for 5 minutes each and incubated with a fluorescently labeled secondary antibody (e.g., Alexa Fluor 488/594, 1:500) for 1 hour, protected from light. Nuclear staining was performed using DAPI (1 μg/mL), and fluorescence signals were observed under a fluorescent microscope to assess the effect of exosomes on M2 polarization.

*Flow cytometry*

To further confirm the M2 polarization state of RAW264.7 cells, flow cytometry was employed to detect the expression levels of CD206 and F4/80. Treated RAW264.7 cells were digested with 0.25% trypsin for 5 minutes, neutralized with culture medium, and collected. The cells were washed twice with PBS and centrifuged at 300 × g to collect the pellet, which was then resuspended in PBS containing 1% BSA as the staining buffer. For each sample, $1 \times 10^6$ cells were first incubated with anti-mouse CD16/CD32 antibodies (1:200) for 15 minutes to block non-specific binding, followed by incubation with CD206-FITC (1:100) and F4/80-PE (1:100) antibodies for 30 minutes in the dark. After incubation, cells were washed twice with PBS and resuspended in PBS for analysis using a flow cytometer (BD FACSCanto II), with each sample acquiring at least 10,000 cells. FlowJo software was used to analyze the data, excluding debris and dead cells, and to determine the proportion of CD206 and F4/80 double-positive cells, which reflects the M2 polarization status of RAW264.7 cells after IL-4 treatment.

*Western blotting*

Total proteins were extracted from rat spinal cord tissues and BV2 cells, and protein concentrations were determined using the BCA assay to ensure equal loading of samples. Equal amounts of protein samples (typically 30-50 μg) were subjected to SDS-PAGE electrophoresis. After electrophoresis, proteins were transferred to PVDF membranes via wet transfer. The membranes were blocked with 5% BSA or 5% skimmed milk at room temperature for 1 hour to prevent non-specific binding. Membranes were then incubated overnight at 4°C with primary antibodies targeting the following proteins: TLR4, p-p65, p65, p-IκBα, IκBα, iNOS (M1 marker), Arg-1 (M2 marker), CD86 (M1 marker), and CD206 (M2 marker), p-p38, and p38.

After primary antibody incubation, membranes were washed three times with PBST (PBS with 0.1% Tween-20) for 5 minutes each. Secondary antibodies conjugated with HRP (diluted 1:5,000 to 1:10,000) were applied and incubated at room temperature for 1 hour. Following secondary antibody incubation, membranes were washed three times with PBST. Protein bands were visualized using ECL chemiluminescence detection. β-actin or GAPDH served as loading controls to ensure equal protein loading across samples. ImageJ software was used to analyze the grayscale values of each protein band, and the expression levels of target proteins were calculated relative to the loading control, presenting results as relative expression levels.

*Quantitative real-time PCR (qRT-PCR)*

Total RNA was extracted from treated BV2 cells, and reverse transcription was performed using a reverse transcription kit to synthesize cDNA. Real-time quantitative PCR was conducted to measure the mRNA expression levels of M1-related genes (iNOS, TNF-α) and M2-related genes (Arg-1, IL-10). The PCR reaction volume was 20 μL, with the following cycling conditions:

initial denaturation at 95°C for 10 minutes, followed by 40 cycles of 95°C for 30 seconds and 60°C for 30 seconds. GAPDH was used as the internal reference gene. Relative gene expression levels were calculated using the 2^-ΔΔCt method.

*Pathway specificity verification grouping*

To confirm the involvement of reactive oxygen species (ROS) and mitogen-activated protein kinase (MAPK) signaling in LPS-induced M1 polarization, BV2 microglia were subjected to selective pharmacological inhibition prior to LPS exposure. For ROS pathway inhibition, cells were pre-incubated with 10 mM N-acetylcysteine (NAC) for 1 h before LPS challenge. NAC functions as an antioxidant, suppressing intracellular ROS generation, thereby allowing assessment of ROS contribution to the polarization process. For MAPK pathway assessment, a separate cohort of BV2 cultures was exposed to 10 μM SB203580 - a selective p38 MAPK inhibitor - for 1 h preceding LPS stimulation. This compound blocks p38 MAPK activation, providing a means to evaluate its role in promoting the M1 phenotype. Following each treatment regimen, total protein was extracted from the cells, and Western blotting was performed according to established protocols to quantify pathway-related and.

*Statistical analysis*

All data were analyzed using GraphPad Prism 8.0 and results were presented as mean ± standard deviation (Mean ± SD). Intergroup comparisons were performed using independent samples t-tests (for two groups) or one-way analysis of variance (ANOVA) followed by Tukey's multiple comparison test. For repeated measurements across multiple time points within the same group, repeated measures ANOVA was applied, and Bonferroni's post hoc test was used for pairwise comparisons. A *P*-value of $< 0.05$ was considered statistically significant.

## Results

*IL-4 treatment successfully induced M2 polarization in RAW264.7 macrophages*

After IL-4 treatment, RAW264.7 macrophages were successfully polarized to the M2 phenotype. Flow cytometry results showed a significant increase in the proportion of CD206 and F4/80 double-positive cells in the IL-4-treated group compared to the control group (**Figure 1A**), indicating IL-4-induced M2 polarization. ELISA results demonstrated that IL-4 treatment significantly elevated the secretion levels of M2-specific factors IL-10, Arg-1, and vascular endothelial growth factor (VEGF) (**Figure 1B**). Immunofluorescence staining further validated these findings, showing markedly enhanced fluorescence intensity of CD206 (**Figure 1C**) and Arg-1 (**Figure 1D**) after IL-4 treatment, confirming the upregulation of M2 markers in RAW264.7 cells.

*Successful extraction and characterization of exosomes from M2-polarized macrophages*

TEM revealed that the extracted exosomes exhibited the typical double-layer membrane structure with diameters ranging from approximately 50-150 nm and maintained intact morphology (**Figure 2A**). NTA further confirmed their size distribution, showing a predominant peak at ~100 nm (**Figure 2B**), consistent with the characteristic dimensions of exosomes. Western blot analysis of exosome-specific markers CD63, CD81, and TSG101, along with the endoplasmic reticulum marker Calnexin, showed strong signals for CD63, CD81, and TSG101, with only a weak band for Calnexin, indicating minimal contamination by other cellular components and confirming the successful isolation of exosomes (**Figure 2C**).

*Exosomes promoted M2 polarization of BV2 microglial cells*

Immunofluorescence staining results showed that PKH67-labeled exosomes (red fluorescence) were successfully internalized by BV2 microglial cells (**Figure 3A**). DAPI (blue) was used for nuclear staining, and the merged images clearly showed the red fluorescence localized within the cytoplasm, confirming exosome uptake. Bar graph results further demonstrated the regulatory effect of exosomes on microglial polarization. The expression of M1-related proteins iNOS, CD80, and CD86 was significantly upregulated in the LPS-treated group, whereas their expression was markedly downregulated in the LPS + Exosome-treated group (**Figure 3B**), indicating that exosomes inhibited LPS-induced M1 polarization. Con-

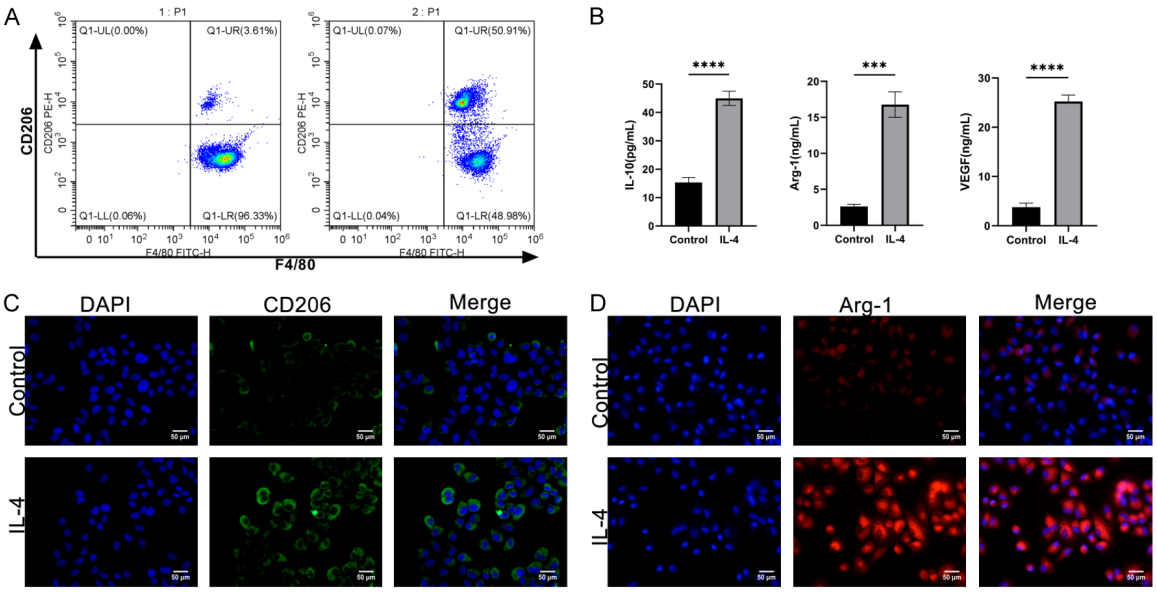


**Figure 1.** IL-4 induced M2 polarization in RAW264.7 macrophages. A. Flow cytometry analysis of CD206 and F4/80 expression in RAW264.7 cells after IL-4 treatment. The proportion of CD206 and F4/80 double-positive cells significantly increased in the IL-4-treated group compared to the control group. B. ELISA analysis showing elevated levels of IL-10, Arg-1, and VEGF in the IL-4-treated group. C. Immunofluorescence staining of CD206 demonstrating increased fluorescence intensity after IL-4 treatment (× 400). D. Immunofluorescence staining of Arg-1 showing enhanced fluorescence intensity in the IL-4-treated group (× 400). Note: Cluster of differentiation 206 (CD206), Cluster of differentiation 80 (F4/80), Interleukin-4 (IL-4), Arginase 1 (Arg-1), Vascular endothelial growth factor (VEGF), Enzyme-linked immunosorbent assay (ELISA), Fluorescent dye PKH67 (PKH67), 4',6-diamidino-2-phenylindole (DAPI). Data are representative of three independent experiments. *P < 0.05 vs. control.

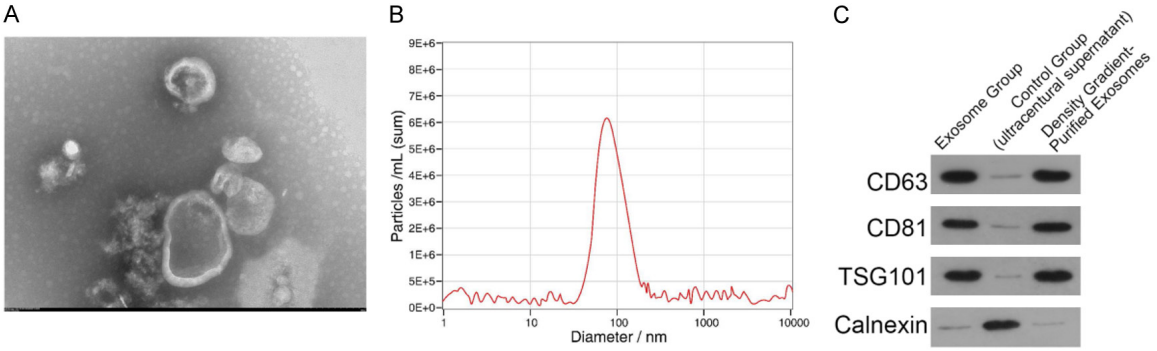


**Figure 2.** Characterization of exosomes derived from M2-polarized RAW264.7 macrophages. A. Transmission electron microscopy (TEM) image showing the morphology of the isolated exosomes with a typical double-layer membrane structure (× 30000). *Scale bar: 50 nm*. B. Nanoparticle tracking analysis (NTA) of exosome size distribution, with the majority of particles around 100 nm in diameter. C. The expression of exosome-specific markers CD63, CD81, TSG101, and the endoplasmic reticulum marker Calnexin was analyzed by Western blot (n=3). Note: Transmission electron microscopy (TEM), Nanoparticle tracking analysis (NTA), Cluster of differentiation 63 (CD63), Cluster of differentiation 81 (CD81), Tumor susceptibility gene 101 (TSG101), Endoplasmic reticulum marker Calnexin, Western blot (WB).

versely, the expression levels of M2-related proteins CD206 and Arg-1 were significantly upregulated in the LPS + Exosome group compared to the LPS group, suggesting that exosomes promoted BV2 microglial cell polarization toward the M2 phenotype (**Figure 3C**).

*Exosomes enhanced BV2 microglial cell proliferation and survival and modulated M1/M2-related gene expression*

Exosome treatment significantly enhanced the proliferation and survival rates of BV2 microgli-

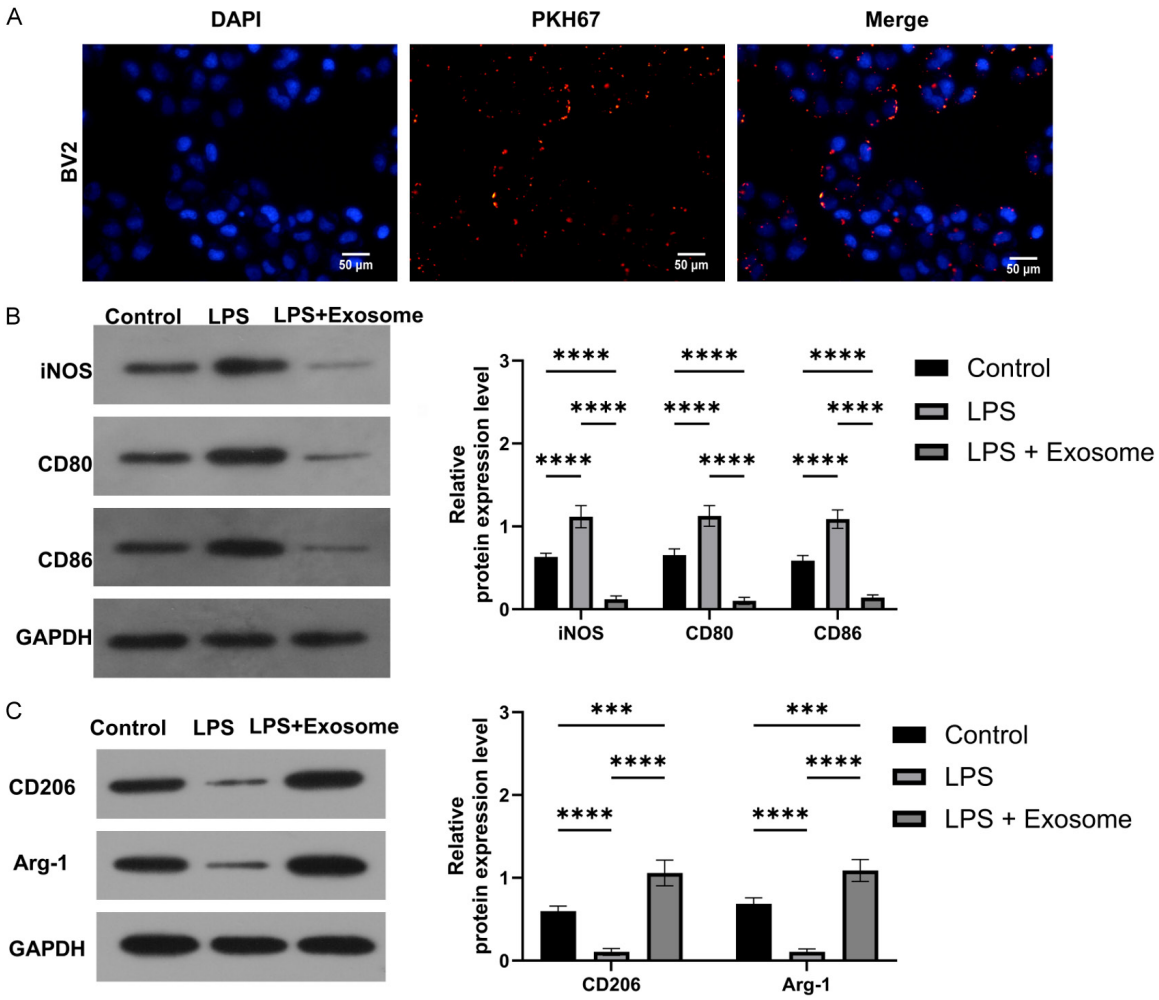


**Figure 3.** Exosome uptake by BV2 microglial cells and its effect on M1/M2 polarization. A. Immunofluorescence staining showing the uptake of PKH67-labeled exosomes (red) by BV2 microglial cells. The nuclei were stained with DAPI (blue). The merged image confirms the internalization of exosomes into the cells (× 400). B. Bar graph displaying the expression levels of M1-related proteins (iNOS, CD80, CD86) in the Control, LPS, and LPS + Exosome groups. LPS treatment significantly increased M1-associated protein expression, while exosome treatment reduced these levels. C. Bar graph showing the expression levels of M2-related proteins (CD206, Arg-1). Exosome treatment significantly upregulated M2-related protein expression compared to the Control and LPS groups. Note: BV2 (a microglial cell line), Inducible nitric oxide synthase (iNOS), Cluster of differentiation 80 (CD80), Cluster of differentiation 86 (CD86), Cluster of differentiation 206 (CD206), Arginase 1 (Arg-1), Lipopolysaccharide (LPS), Standard deviation (SD). Data are presented as mean ± SD. ****P < 0.0001, ***P < 0.001 vs. Control group (n=3).

al cells. CCK-8 assay results indicated that the proliferation capacity of cells in the LPS + Exosome group was significantly higher than that in the LPS group at 24 hours, 48 hours, and 72 hours (**Figure 4A**), approaching or exceeding the proliferation levels of the control group. Colony formation assays further supported these finding, showing a significantly greater number of colonies in the LPS + Exosome group compared to the LPS group, indicating that exosomes effectively improved the survival rate of cells subjected to LPS-induced stress (**Figure 4B**).

qRT-PCR results revealed that the expression of M2 marker genes Arg-1 and IL-10 was significantly upregulated, while the expression of M1 marker genes iNOS and TNF-α was significantly downregulated in the LPS + Exosome group compared to the LPS group (**Figure 4C**, **4D**). These findings suggest that exosomes enhance BV2 microglial proliferation and survival while

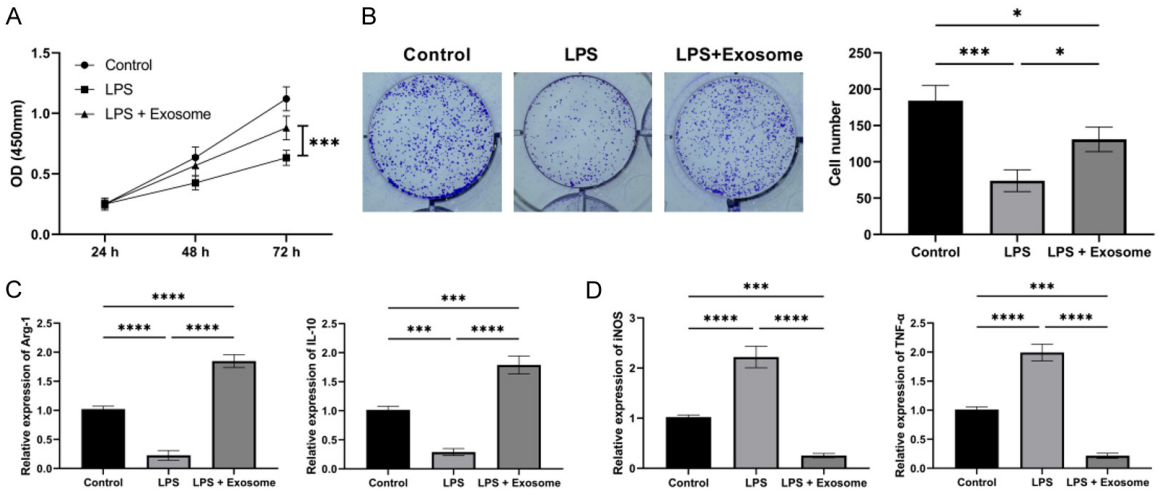


**Figure 4.** Exosomes promoted BV2 microglial cell proliferation and survival, and modulated M1/M2-related gene expression. A. CCK-8 assay showing the proliferation of BV2 cells at 24 h, 48 h, and 72 h. The LPS + Exosome group exhibited significantly higher proliferation compared to the LPS group. B. Colony formation assay indicating the number of BV2 cells in each group. Exosome treatment improved the survival of BV2 cells, as shown by the increased number of colonies in the LPS + Exosome group compared to the LPS group. C. qRT-PCR analysis of M2-related genes (Arg-1, IL-10) showing significant upregulation in the LPS + Exosome group compared to the LPS group. D. qRT-PCR analysis of M1-related genes (iNOS, TNF-α) showing significant downregulation in the LPS + Exosome group. Note: Cell counting kit-8 (CCK-8), Quantitative reverse transcription polymerase chain reaction (qRT-PCR), M1 (classically activated microglia), M2 (alternatively activated microglia), Tumor necrosis factor-alpha (TNF-α), Interleukin-10 (IL-10). Data are presented as mean ± SD. ****P < 0.0001, ***P < 0.001, **P < 0.01, *P < 0.05 vs. Control or LPS group (n=3).

modulating their polarization state by inhibiting pro-inflammatory M1 genes and promoting anti-inflammatory M2 genes.

*Exosomes regulated protein expression and suppressed the TLR4/NF-κB signaling pathway in BV2 microglial cells*

Exosome treatment significantly modulated protein expression and NF-κB signaling activity in BV2 microglial cells. Western blot analysis revealed that the expression levels of TLR4, p-p65, and p-IκBα were markedly upregulated in the LPS-treated group, indicating activation of the TLR4/NF-κB pathway (**Figure 5A**). However, in the LPS + Exosome group, the expression of these proteins was significantly reduced, suggesting that exosomes inhibited LPS-induced TLR4/NF-κB pathway activation. Additionally, the expression of IκBα was significantly decreased in the LPS group but was restored in the LPS + Exosome group, further demonstrating the inhibitory effect of exosomes on inflammatory signaling. ELISA results showed that LPS treatment significantly increased the secretion levels of inflammatory cytokines IL-6, TNF-α, and MCP-1 (**Figure 5B**), whereas exosome treatment markedly reduced their levels, further demonstrating the inhibitory effects of exosomes on inflammatory responses.

*Exosomes treatment alleviated bone cancer pain and modulated M1/M2 polarization in the spinal cord of rats*

The PWT test indicated that rats in the BCP group had a significantly reduced PWT, reflecting increased mechanical pain sensitivity. However, in the BCP + Exosome group, the PWT was significantly elevated, demonstrating that exosomes effectively reduced pain sensitivity (**Figure 6A**). WB analysis revealed that the expression of M1 marker CD86 was significantly upregulated in the spinal cords of BCP rats, whereas exosome treatment significantly decreased CD86 expression, indicating inhibition of M1 polarization (**Figure 6B**). Additionally, the expression of the M2 marker CD206 was lower in the BCP group compared to the Sham group but significantly upregulated in the BCP + Exo group, suggesting that exosomes promoted M2 polarization and regulated the inflammatory response (**Figure 6C**).

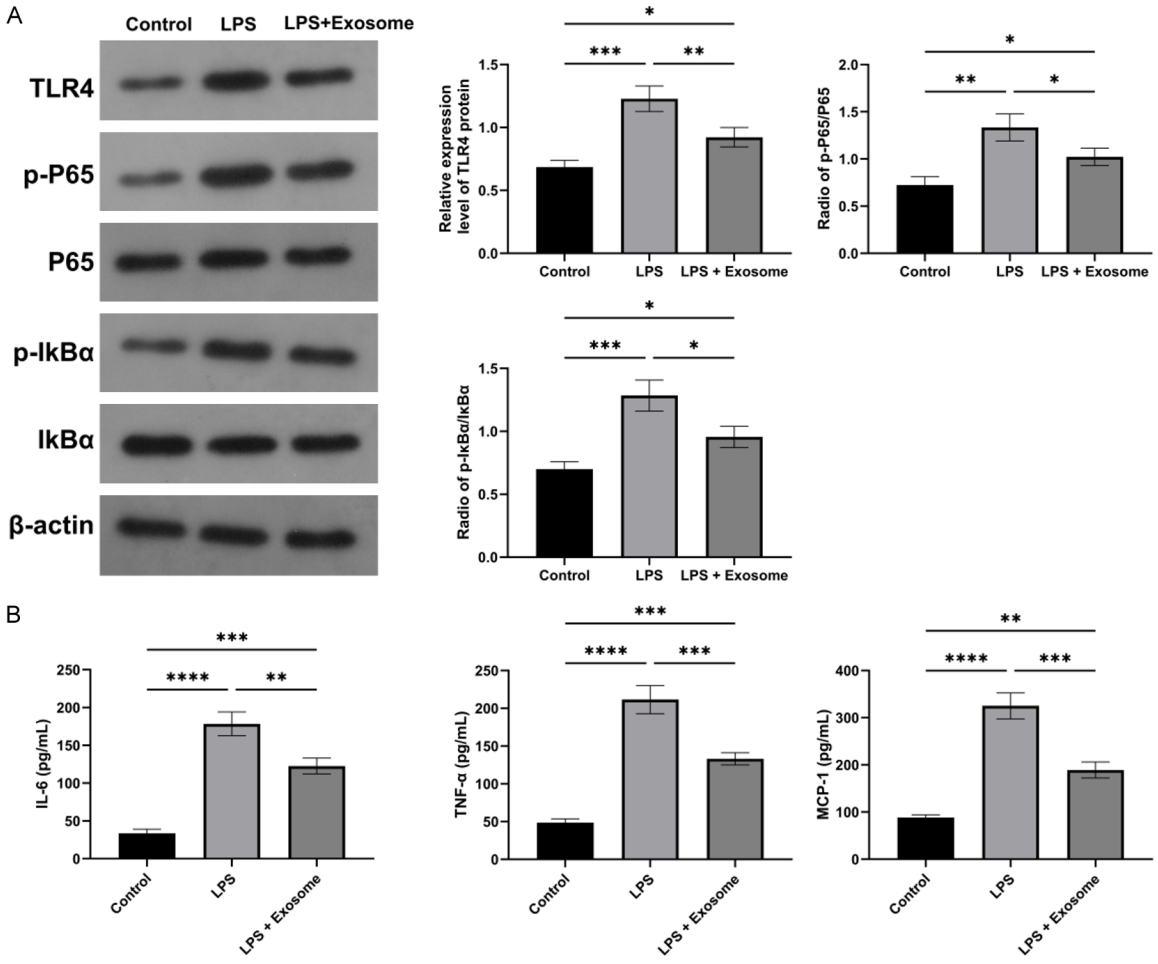


**Figure 5.** Exosomes suppressed TLR4/NF-κB signaling pathway related protein expression in BV2 microglial cells. A. Western blot analysis of TLR4, p-p65, p65, p-IκBα, and IκBα protein expression in BV2 microglial cells. LPS treatment significantly increased the expression of TLR4, p-p65, and p-IκBα, indicating activation of the TLR4/NF-κB pathway. Exosome treatment in the LPS + Exosome group reduced the expression of these proteins. β-actin was used as an internal control. B. ELISA analysis of inflammatory cytokines (IL-6, TNF-α, MCP-1) in the culture supernatants of BV2 cells. LPS treatment significantly increased the levels of these cytokines, while exosome treatment reduced their expression. Note: Toll-like receptor 4 (TLR4), Phosphorylated p65 (p-p65), p65 subunit of nuclear factor kappa-light-chain-enhancer of activated B cells (p65), Phosphorylated inhibitor of κB alpha (p-IκBα), Inhibitor of κB alpha (IκBα), Nuclear factor kappa-light-chain-enhancer of activated B cells (NF-κB), Enzyme-linked immunosorbent assay (ELISA). Data are presented as mean ± SD. ****P < 0.0001, ***P < 0.001, **P < 0.01, *P < 0.05 vs. Control or LPS group (n=3).

*Exosomes regulated M1/M2 polarization and the TLR4/NF-κB signaling pathway in the spinal cord of rats with bone cancer pain*

To verify the coexistence of macrophages and microglia in the BCP model, F4/80 (macrophage marker) and Iba1 (microglial marker) protein expression in the spinal dorsal horn was analyzed by Western blot (**Figure 7A**). Both F4/80 and Iba1 levels were significantly increased in the BNT group compared to the Sham group, indicating enhanced macrophage infiltration and microglial activation. Exosome treatment significantly reduced F4/80 and Iba1 levels compared to the BNT group (**Figure 7B**), suggesting that exosomes attenuated macrophage recruitment and microglial reactivity specifically in the spinal dorsal horn. To verify the localization of exosomes in the BCP model, double immunofluorescence staining was performed on spinal cord tissues. PKH67-labeled exosomes (green fluorescence) were clearly

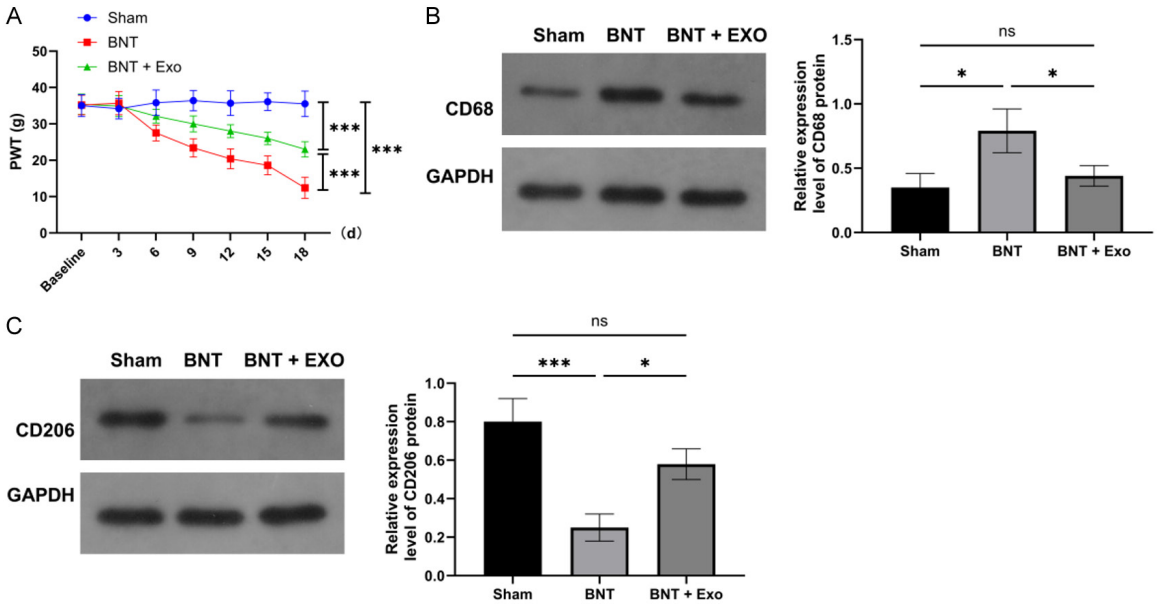


**Figure 6.** Exosomes alleviated bone cancer pain and modulated M1/M2 polarization in the spinal cord of rats. A. Paw withdrawal threshold (PWT) test showing that BCP rats exhibited significantly lower PWT values, indicating heightened mechanical pain sensitivity. Exosome treatment significantly increased PWT values, reducing pain sensitivity. B. WB of the M1 marker CD86 in the spinal cord, showing significantly higher expression in the BCP group compared to the Sham group, while exosome treatment reduced CD86 expression. C. WB of the M2 marker CD206, showing lower expression in the BCP group and significantly increased expression after exosome treatment. Note: Paw withdrawal threshold (PWT), Bone cancer pain model (BNT), Control group (Sham), Western blot (WB). Data are presented as mean ± SD. ***P < 0.001, *P < 0.05 vs. Sham or BCP group (n=3).

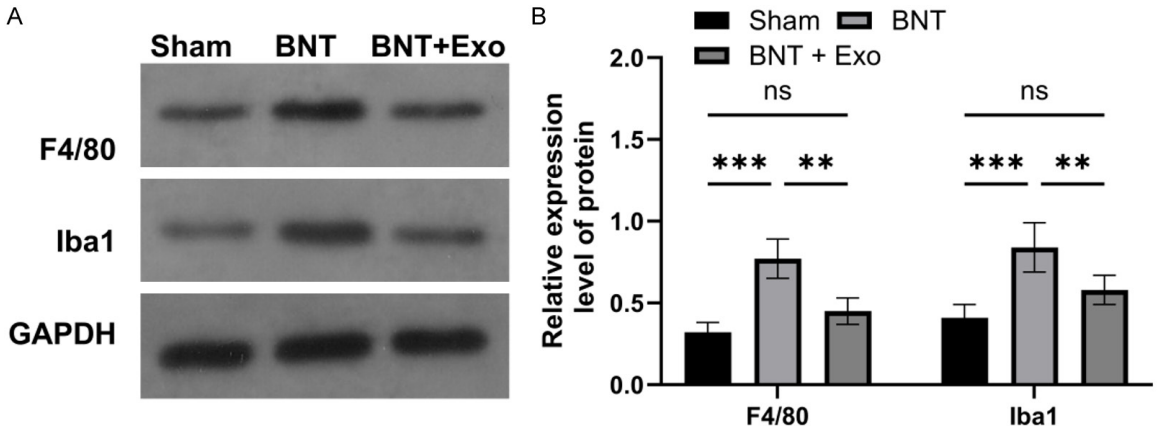


**Figure 7.** Exosomes modulated F4/80 and Iba-1 expression in the spinal cord of rats with bone cancer pain. A. Protein band of F4/80, Iba-1 in spinal cord sections of Sham, BCP and BCP + Exo groups. B. Quantified result of protein levels of F4/80 and Iba-1. Note: Macrophage marker F4/80 (F4/80), Ionized calcium-binding adaptor molecule 1 (Iba-1), Western blot (WB). Data are presented as mean ± SD. ***P < 0.001,**P < 0.01, vs. Sham or BCP group (n=3).

detected within microglia and macrophages in the BCP + Exo group, with prominent signals in the gray matter region (**Figure 8A**). WB further revealed M1 markers (iNOS, CD86, CD68) were significantly upregulated in the BCP group, reflecting cancer-induced M1 polarization (**Figure 8B**). In contrast, exosome treatment markedly suppressed these M1 markers (**Figure 8C**). Additionally, M2 markers (CD206, Arg-1), which were downregulated in the BCP group, were significantly restored in the BCP + Exosome group (**Figure 8C**), demonstrating

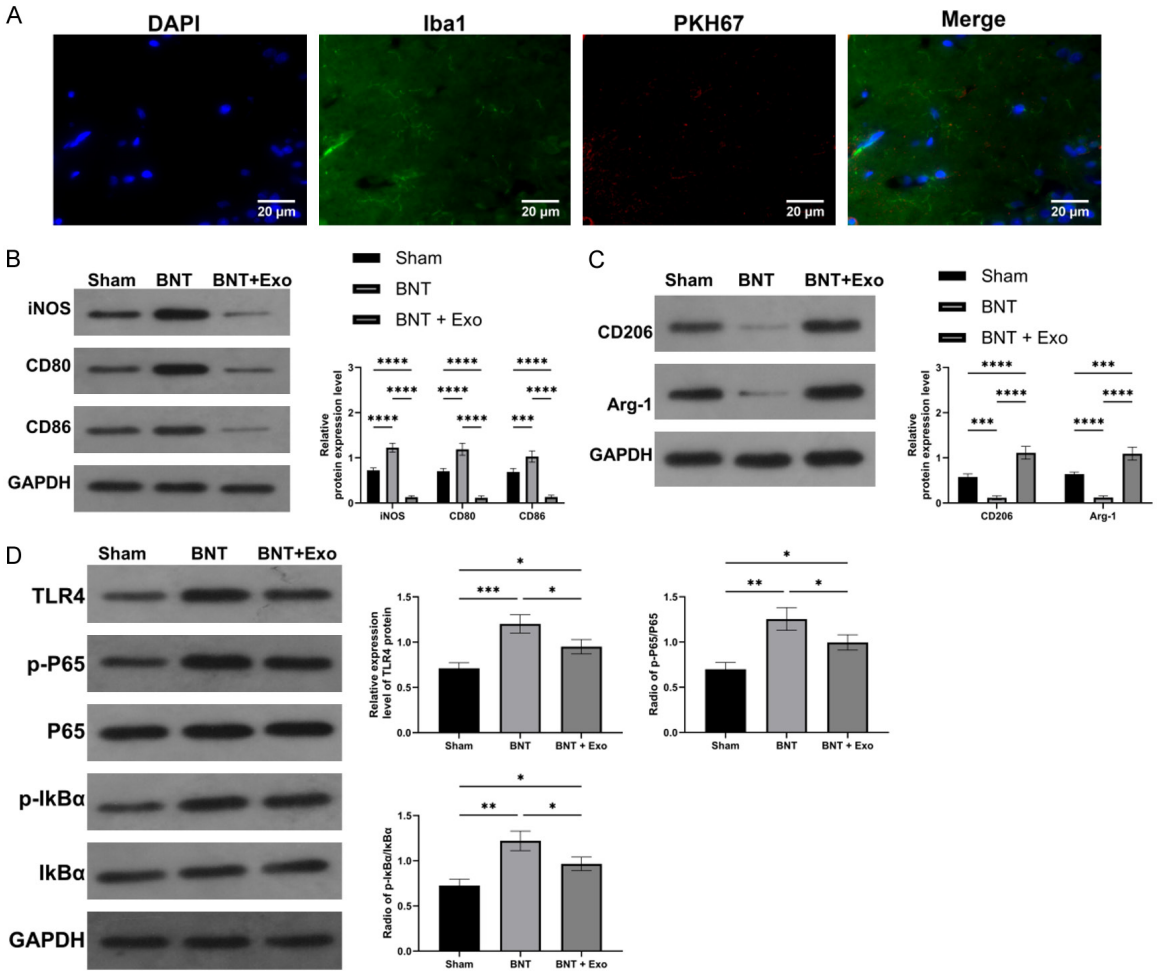


**Figure 8.** Exosomes regulated M1/M2 polarization and the TLR4/NF-κB signaling pathway in the spinal cord of rats with bone cancer pain. A. Immunofluorescence staining showing the localization and internalization of red PKH67-labeled exosomes (red) in microglia and macrophages in the gray matter region of the spinal cord. Nuclei were stained with DAPI (blue), and merged images confirm exosome uptake in the BCP + Exo group (× 600). B. Western blot analysis of M1 polarization markers (iNOS, CD86, CD68) in the Sham, BCP , and BCP + Exo groups. M1 markers were significantly upregulated in the BCP group, while exosome treatment reduced their expression. C. Western blot analysis of M2 polarization markers (CD206, Arg-1). M2 markers were downregulated in the BCP group, and exosome treatment significantly upregulated their expression. D. Western blot analysis of TLR4, p-p65, and p-IκBα. The TLR4/NF-κB pathway was activated in the BCP group, and exosome treatment inhibited the activation of this pathway. Note: Inducible nitric oxide synthase (iNOS), Cluster of differentiation 86 (CD86), Cluster of differentiation 206 (CD206), Arginase 1 (Arg-1), Phosphorylated p65 (p-p65), Phosphorylated inhibitor of κB alpha (p-IκBα), Lipopolysaccharide (LPS), Western blot (WB). Data are presented as mean ± SD. ****P < 0.0001, ***P < 0.001, **P < 0.01, *P < 0.05 vs. Sham or BCP group (n=3).

exosome-mediated promotion of M2 polarization. Regarding the TLR4/NF-κB pathway, spinal dorsal horn tissues from BCP rats exhibited elevated expression of TLR4, p-p65, and p-IκBα, indicating pathway activation (**Figure 8D**). However, these proteins were significantly downregulated in the BNT + Exo group (**Figure 8D**), confirming that exosomes inhibited TLR4/NF-κB signaling in the spinal cord of rats with BCP (Figure S1).

## Discussion

BCP is among the most prevalent and challenging chronic pain syndromes in patients with advanced malignancies, exerting a profound negative impact on quality of life [18, 19]. Increasing evidence suggests that microglial activation is central to both the onset and persistence of BCP, with polarization toward M1 or M2 phenotypes dictating their pro- or anti-

inflammatory functions [20]. M1-polarized microglia exacerbate nociception by releasing pro-inflammatory cytokines, including TNF-α, IL-1β, and IL-6, thereby amplifying neuroinflammation and neuronal injury [21]. In contrast, M2-polarized microglia counteract this effect by secreting anti-inflammatory mediators, such as IL-10 and TGF-β, which suppress inflammatory signaling and promote tissue repair [22, 23].

Exosomes, increasingly recognized as pivotal mediators of intercellular communication, have been implicated in modulating immune cell polarization and influencing inflammatory processes within both tumor microenvironments and other pathological settings [24, 25]. In our study, macrophage-derived exosomes significantly reduced M1 microglial polarization while enhancing M2 polarization, ultimately attenuating BCP. This effect was largely attributable to their ability to modulate the TLR4/NF-κB signaling pathway, resulting in the downregulation of pro-inflammatory cytokines and suppression of excessive inflammatory activity. These observations add to a growing body of evidence emphasizing the immunomodulatory potential of exosomes. For example, Arabpour et al. [24] summarized that mesenchymal stem cell-derived exosomes promote M2 macrophage polarization, exerting robust anti-inflammatory effects in a variety of inflammatory diseases. Similarly, Wang et al. [25] demonstrated that exosomes released from M2 macrophages facilitated diabetic fracture healing by modulating the bone immune milieu. Conversely, Lu et al. [26] showed that M2 macrophage-derived exosomes could also enhance hepatocellular carcinoma metastasis by delivering miR-23a-3p, underscoring their potential impact-either beneficial or deleterious-depending on the disease context.

Our data further suggest that these exosomes may carry functional miRNAs or proteins capable of modulating TLR4/NF-κB activation in microglia. Since this signaling axis is known to favor M1 polarization and drive pro-inflammatory cytokine release, its suppression offers a plausible mechanism for the observed analgesic effects. This aligns with the findings of Zhong et al. [27], who reported that curcumin reduced IL-6, TNF-α, and MCP-1 secretion in THP-1 cells via inhibition of the TLR4/NF-κB/miR-33a pathway. Similarly, Li et al. [28], demonstrated that paeoniflorin relieved neuropathic pain by modulating microglial polarization through the RhoA/p38 MAPK cascade. Additional support comes from Wu et al. [29], who identified the P2X7 receptor as a mediator of spinal microglial M1 polarization in cancer-induced bone pain, with receptor inhibition both promoting M2 polarization and relieving pain symptoms.

Other mechanistic insights have been reported: Fei et al. [30] demonstrated that p53 lysine lactylation under hypoxic conditions promotes pro-inflammatory BV2 activation via NF-κB, while He et al. [22] showed that miR-155-5p regulates mechanical hypersensitivity in a rat BCP model by targeting transcription factor 4 in spinal neurons. Collectively, these studies reinforce the concept that exosomes influence microglial polarization through diverse molecular routes, thereby shaping the inflammatory landscape and contributing to pain modulation in BCP.

The clinical significance of this work lies in demonstrating the promise of macrophage-derived exosomes as a new class of biological therapeutics. Owing to their excellent biocompatibility and low immunogenicity, exosomes can cross biological barriers and deliver functional cargos directly to target cells. Such properties make them attractive candidates for innovative strategies in managing BCP, especially for patients with chronic pain refractory to conventional treatments. For example, Ma et al. [31] engineered exosomes by fusing M2-type macrophages with bone marrow mesenchymal stem cells, enabling targeted delivery to bone resorption sites and modulation of macrophage polarization-highlighting the feasibility of tailoring exosomes for bone-related pathologies.

Nonetheless, several limitations should be acknowledged. First, the relatively small sample size may constrain the statistical robustness of our conclusions. Second, while the *in vitro* and *in vivo* models employed recapitulate certain aspects of BCP, they cannot fully capture the complexity of the human condition. Third, technical challenges in exosome isolation and purification could affect yield consistency and, consequently, therapeutic efficacy. Future research should focus on identifying the precise molecular constituents-such as specific miRNAs or proteins-within exosomes that

modulate the TLR4/NF-κB axis. Additionally, larger-scale animal experiments and rigorously designed clinical trials are needed to confirm the safety and efficacy of exosome-based therapies. Exploring combinatorial strategies that integrate exosome therapy with other treatment modalities could further elucidate potential synergistic effects and provide comparative therapeutic advantages.

## Conclusion

Our findings demonstrate that macrophage-derived exosomes can effectively attenuate BCP through modulation of the TLR4/NF-κB signaling pathway. This mechanism involves suppression of M1 microglial polarization, enhancement of M2 polarization, and consequent reduction in pro-inflammatory cytokine production. Furthermore, alterations in microglial polarization status and inhibition of TLR4/NF-κB activation within spinal cord tissue provide further evidence supporting the analgesic potential of exosome therapy in BCP.

## Acknowledgements

This work was supported by the National Natural Science Foundation of China [grant number 82160229].

## Disclosure of conflict of interest

None.

**Address correspondence to:** Weixing Ding, Department of Pain, Qujing Second People's Hospital, No. 289 Qilin Xi Road, Qilin District, Qujing 655009, Yunnan, China. E-mail: dwx466145142@163.com; Zhangxiang Huang, Department of Pain, First Affiliated Hospital of Kunming Medical University, Kunming 650000, Yunnan, China. E-mail: adams7777@163.com

## References

[1] Hamash K and Walker SL. Comprehensive clinical literature review of managing bone metastases in breast cancer: focus on pain and skeletal-related events. Clin J Oncol Nurs 2023; 27: 615-628.

[2] Yang Y, Yang W, Zhang R and Wang Y. Peripheral mechanism of cancer-induced bone pain. Neurosci Bull 2024; 40: 815-830.

[3] Diaz-delCastillo M, Hansen RB, Appel CK, Nielsen L, Nielsen SN, Karyniotakis K, Dahl LM, Andreasen RB and Heegaard AM. Modulation of rat cancer-induced bone pain is independent of spinal microglia activity. Cancers (Basel) 2020; 12: 2740.

[4] Ni JW, Li CX, Chen XW and Cai WP. Triggering receptor expressed on myeloid cell-2 protects PC12 cells injury by inhibiting BV2 microglial activation. Neurol India 2022; 70: 2378-2382.

[5] Dingyi L, Libin H, Jifeng P, Ding Z, Yulong L, Zhangyi W, Yunong Y, Qinghua W and Feng L. Silencing CXCL16 alleviate neuroinflammation and M1 microglial polarization in mouse brain hemorrhage model and BV2 cell model through PI3K/AKT pathway. Exp Brain Res 2024; 242: 1917-1932.

[6] Xu Q, Kong F, Zhao G, Jin J, Feng S and Li M. SP1 transcriptionally activates HTR2B to aggravate traumatic spinal cord injury by shifting microglial M1/M2 polarization. J Orthop Surg Res 2024; 19: 230.

[7] Xie J, Tuo P, Zhang W and Wang S. Inhibition of the TLR4/NF-κB pathway promotes the polarization of LPS-induced BV2 microglia toward the M2 phenotype. Neuroreport 2023; 34: 834-844.

[8] Zhang J, Zheng Y, Luo Y, Du Y, Zhang X and Fu J. Curcumin inhibits LPS-induced neuroinflammation by promoting microglial M2 polarization via TREM2/ TLR4/ NF-κB pathways in BV2 cells. Mol Immunol 2019; 116: 29-37.

[9] Wang Y, Wei W, Guo M, Li S, Chai Z, Ma C, Jiang Y, Song L and Yu J. [Lycium barbarum polysaccharide promotes M2 polarization of BV2 microglia induced by LPS via inhibiting the TLR4/NF-κB signaling pathway]. Xi Bao Yu Fen Zi Mian Yi Xue Za Zhi 2021; 37: 1066-1072.

[10] Zhao W, Ma L, Deng D, Zhang T, Han L, Xu F, Huang S, Ding Y and Chen X. M2 macrophage polarization: a potential target in pain relief. Front Immunol 2023; 14: 1243149.

[11] Zhou H, Zhou J, Teng H, Yang H, Qiu J and Li X. MiR-145 enriched exosomes derived from bone marrow-derived mesenchymal stem cells protects against cerebral ischemia-reperfusion injury through downregulation of FOXO1. Biochem Biophys Res Commun 2022; 632: 92-99.

[12] Yokoi A and Ochiya T. Exosomes and extracellular vesicles: rethinking the essential values in cancer biology. Semin Cancer Biol 2021; 74: 79-91.

[13] He Z, Wang J, Zhu C, Xu J, Chen P, Jiang X, Chen Y, Jiang J and Sun C. Exosome-derived FGD5-AS1 promotes tumor-associated macrophage M2 polarization-mediated pancreatic cancer cell proliferation and metastasis. Cancer Lett 2022; 548: 215751.

[14] Rao X, Zhou X, Wang G, Jie X, Xing B, Xu Y, Chen Y, Li J, Zhu K, Wu Z, Wu G, Wu C and Zhou R.

NLRP6 is required for cancer-derived exosome-modified macrophage M2 polarization and promotes metastasis in small cell lung cancer. Cell Death Dis 2022; 13: 891.
[15] Qian W, Huang L, Xu Y, Lu W, Wen W, Guo Z, Zhu W and Li Y. Hypoxic ASCs-derived exosomes attenuate colitis by regulating macrophage polarization via miR-216a-5p/HMGB1 axis. Inflamm Bowel Dis 2023; 29: 602-619.
[16] Li X, Yang N, Cheng Q, Zhang H, Liu F and Shang Y. MiR-21-5p in macrophage-derived exosomes targets smad7 to promote epithelial mesenchymal transition of airway epithelial cells. J Asthma Allergy 2021; 14: 513-524.
[17] Khasabova IA, Khasabov SG, Johns M, Juliette J, Zheng A, Morgan H, Flippen A, Allen K, Golovko MY, Golovko SA, Zhang W, Marti J, Cain D, Seybold VS and Simone DA. Exosome-associated lysophosphatidic acid signaling contributes to cancer pain. Pain 2023; 164: 2684-2695.
[18] Kang H, Lee Y and Kim M. Effects of aromatherapy on quality of life and pain in patients with cancer: a meta-analysis. J Pain Symptom Manage 2024; 68: e434-e446.
[19] Shrestha S, Sapkota S, Teoh SL, Kc B, Paudyal V, Lee SWH and Gan SH. Comprehensive assessment of pain characteristics, quality of life, and pain management in cancer patients: a multi-center cross-sectional study. Qual Life Res 2024; 33: 2755-2771.
[20] Huo W, Zhang Y, Liu Y, Lei Y, Sun R, Zhang W, Huang Y, Mao Y, Wang C, Ma Z and Gu X. Dehydrocorydaline attenuates bone cancer pain by shifting microglial M1/M2 polarization toward the M2 phenotype. Mol Pain 2018; 14: 1744806918781733.
[21] Lin SL, Yang SY, Tsai CH, Fong YC, Chen WL, Liu JF, Lin CY and Tang CH. Nerve growth factor promote VCAM-1-dependent monocyte adhesion and M2 polarization in osteosarcoma microenvironment: implications for larotrectinib therapy. Int J Biol Sci 2024; 20: 4114-4127.
[22] He Q, Liu L, Wang Y, Xu C, Xu M, Fu J, Zhu J, Zhao B, Ni C, Yao M, Lin X and Ni H. miR-155-5p in the spinal cord regulates hypersensitivity in a rat model of bone cancer pain. Mol Pain 2022; 18: 17448069221127811.
[23] Zhang X, Li X, Wang W, Zhang Y, Gong Z, Peng Y, Wu J and You X. STING contributes to cancer-induced bone pain by promoting M1 polarization of microglia in the medial prefrontal cortex. Cancers (Basel) 2022; 14: 5188.
[24] Arabpour M, Saghazadeh A and Rezaei N. Anti-inflammatory and M2 macrophage polarization-promoting effect of mesenchymal stem cell-derived exosomes. Int Immunopharmacol 2021; 97: 107823.
[25] Wang Y, Lin Q, Zhang H, Wang S, Cui J, Hu Y, Liu J, Li M, Zhang K, Zhou F, Jing Y, Geng Z and Su J. M2 macrophage-derived exosomes promote diabetic fracture healing by acting as an immunomodulator. Bioact Mater 2023; 28: 273-283.
[26] Lu Y, Han G, Zhang Y, Zhang L, Li Z, Wang Q, Chen Z, Wang X and Wu J. M2 macrophage-secreted exosomes promote metastasis and increase vascular permeability in hepatocellular carcinoma. Cell Commun Signal 2023; 21: 299.
[27] Zhong Y, Liu C, Feng J, Li JF and Fan ZC. Curcumin affects ox-LDL-induced IL-6, TNF-α, MCP-1 secretion and cholesterol efflux in THP-1 cells by suppressing the TLR4/NF-κB/miR33a signaling pathway. Exp Ther Med 2020; 20: 1856-1870.
[28] Li X, Shi H, Zhang D, Jing B, Chen Z, Zheng Y, Chang S, Gao L and Zhao G. Paeonol alleviates neuropathic pain by modulating microglial M1 and M2 polarization via the RhoA/p38MAPK signaling pathway. CNS Neurosci Ther 2023; 29: 2666-2679.
[29] Wu P, Zhou G, Wu X, Lv R, Yao J and Wen Q. P2X7 receptor induces microglia polarization to the M1 phenotype in cancer-induced bone pain rat models. Mol Pain 2022; 18: 17448069211060962.
[30] Fei X, Chen L, Gao J, Jiang X, Sun W, Cheng X, Zhao T, Zhao M and Zhu L. p53 lysine-lactylated modification contributes to lipopolysaccharide-induced proinflammatory activation in BV2 cell under hypoxic conditions. Neurochem Int 2024; 178: 105794.
[31] Ma T, Chen S, Wang J, Liang S, Chen M, Liu Q, Zhang Z, Liu G, Yang Y, Hu Y and Xie J. Enhanced osteolysis targeted therapy through fusion of exosomes derived from m2 macrophages and bone marrow mesenchymal stem cells: modulating macrophage polarization. Small 2024; 20: e2303506.

**Specific role of exosomes in LPS-induced Microglial polarization and its independence from ROS and p38 MAPK pathway interference**

To verify the specific role of exosomes in LPS-induced microglial polarization, we added ROS inhibitor NAC and p38 MAPK inhibitor SB203580 to the exosome treatment groups and observed their effects on M1/M2 polarization. The results showed that, regardless of the addition of NAC or SB203580, exosomes were able to significantly inhibit LPS-induced M1 polarization and promote M2 polarization, and this effect was independent of the ROS or p38 MAPK pathways. In the NAC treatment group, the expression of iNOS and CD86 decreased, while M2 markers CD206 and Arg-1 increased, indicating that NAC inhibited ROS production and alleviated M1 polarization. However, in the LPS + Exosomes + NAC group, the expression of iNOS and CD86 remained at low levels, while M2 markers CD206 and Arg-1 maintained higher levels, suggesting that the effect of exosomes was not significantly interfered with by NAC. Similarly, in the SB203580 treatment group, SB203580 significantly decreased the expression of iNOS and CD86 and promoted M2 polarization. However, in the LPS + Exosomes + SB203580 group, exosomes still effectively inhibited M1 polarization and promoted M2 polarization, with iNOS and CD86 remaining at low levels, while M2 markers CD206 and Arg-1 remained at high levels. These results suggest that the immune regulatory effect of exosomes is independent of ROS or MAPK pathways, further confirming the specific role of exosomes in LPS-induced polarization (Figure S1).

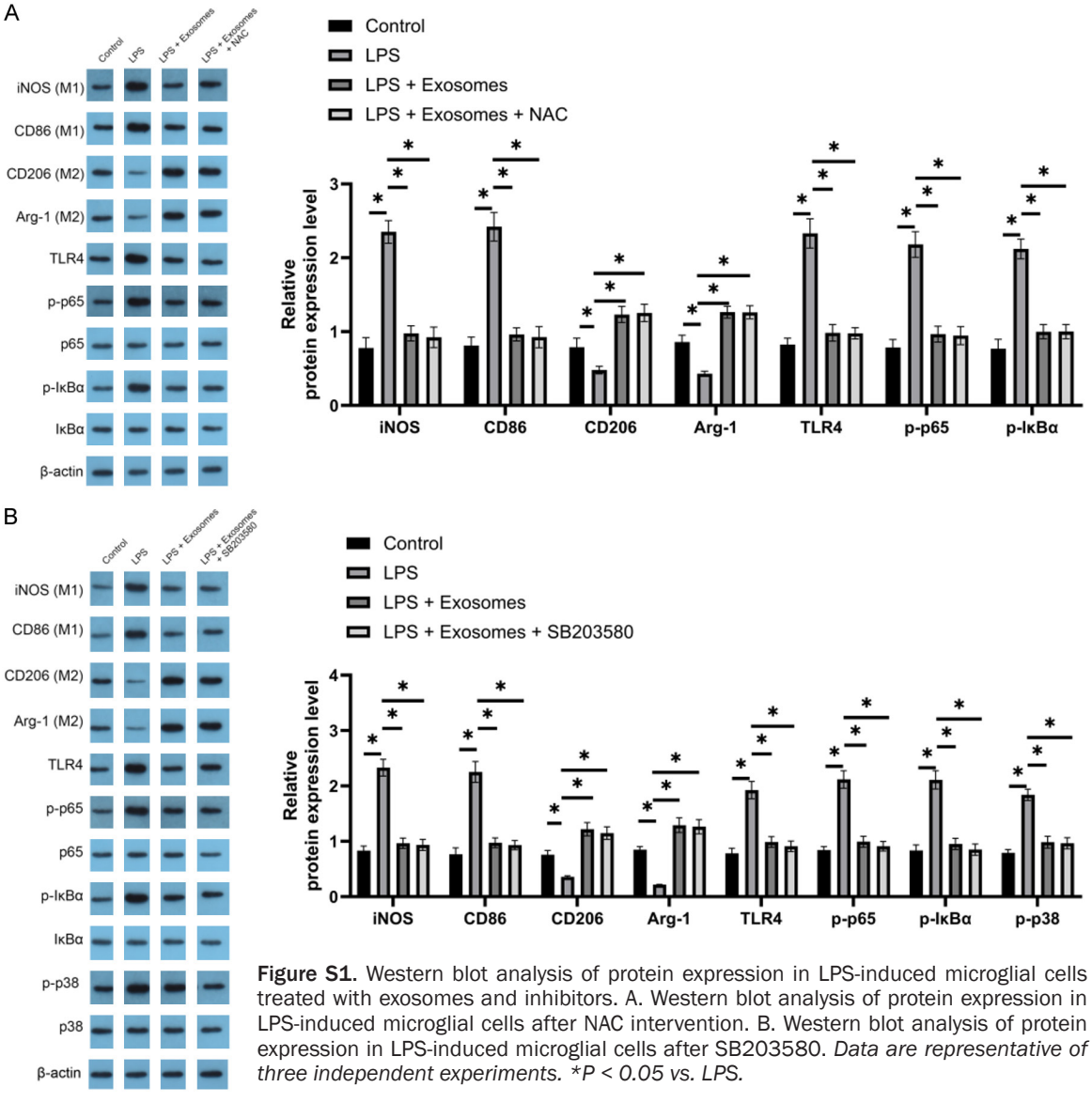


**Figure S1.** Western blot analysis of protein expression in LPS-induced microglial cells treated with exosomes and inhibitors. A. Western blot analysis of protein expression in LPS-induced microglial cells after NAC intervention. B. Western blot analysis of protein expression in LPS-induced microglial cells after SB203580. *Data are representative of three independent experiments. *P < 0.05 vs. LPS.*